JCI insight

# C3($H_2O$) prevents rescue of complement-mediated C3 glomerulopathy in *Cfh*$^{-/-}$ *Cfd*$^{-/-}$ mice

Yuzhou Zhang, … , Ronald P. Taylor, Richard J.H. Smith

*JCI Insight.* 2020;5(9):e135758. https://doi.org/10.1172/jci.insight.135758.

Research Article Nephrology

## Graphical abstract

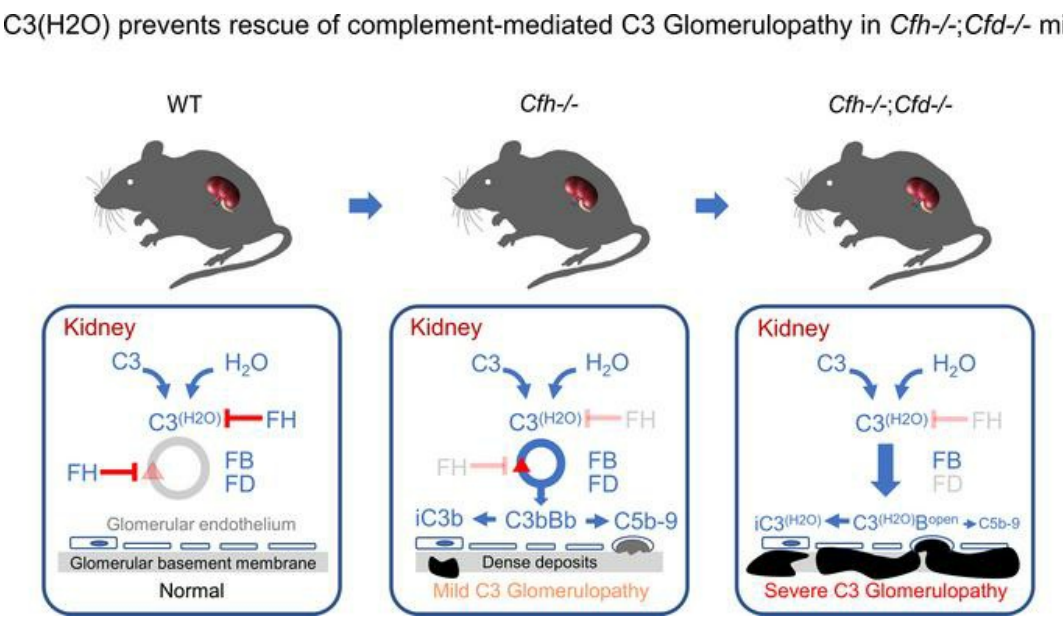

JCI insight

RESEARCH ARTICLE

# C3($H_2O$) prevents rescue of complement-mediated C3 glomerulopathy in *Cfh*$^{-/-}$ *Cfd*$^{-/-}$ mice

**Yuzhou Zhang,[1] Adam Keenan,[1] Dao-Fu Dai,[2] Kristofer S. May,[1] Emily E. Anderson,[1] Margaret A. Lindorfer,[3] John B. Henrich,[1] Gabriella R. Pitcher,[1] Ronald P. Taylor,[3] and Richard J.H. Smith[1]**

[1]Molecular Otolaryngology and Renal Research Laboratories, and [2]Department of Pathology, Carver College of Medicine, University of Iowa, Iowa City, Iowa, USA. [3]Department of Biochemistry and Molecular Genetics, University of Virginia School of Medicine, Charlottesville, Virginia, USA.

**Therapeutic complement inhibition is a major focus for novel drug development. Of upstream targets, factor D (FD) is appealing because it circulates in plasma at low concentrations and has a single function: to cleave factor B to generate C3 convertase of the alternative pathway (AP). Mice with a targeted deletion of factor H (FH; *Cfh*$^{-/-}$ mice) develop C3 glomerulopathy (C3G) due to uncontrolled AP activity. To assess the impact of FD inhibition, we studied *Cfh*$^{-/-}$ *Cfd*$^{-/-}$ mice. We show that C3G in *Cfh*$^{-/-}$ mice is not rescued by removing FD. We used serum from *Cfh*$^{-/-}$ *Cfd*$^{-/-}$ mice to demonstrate that residual AP function occurs even when both FD and FH are missing and that hemolytic activity is present due to the action of C3($H_2O$). We propose that uncontrolled tick-over leads to slow activation of the AP in *Cfh*$^{-/-}$ *Cfd*$^{-/-}$ mice and that a minimal threshold of FH is necessary if tissue deposition of C3 is to be prevented. The FD/FH ratio dictates serum C3 level and renal C3b deposition. In C3G patients with chronic renal disease, the FD/FH ratio correlates inversely with C3 and C5 serum levels, suggesting that continuous AP control may be difficult to achieve by targeting FD.**

## Introduction

Therapeutic complement inhibition using eculizumab, a humanized anti-C5 mAb, was introduced for the treatment of paroxysmal nocturnal hemoglobinuria (PNH) in 2002 (1, 2). Five years later, the US Food and Drug Administration (FDA) approved eculizumab as a first-in-class complement inhibitor for PNH, thereby validating the concept of complement inhibition as an effective clinical therapy (3). In 2011, the FDA also licensed eculizumab for the treatment of the ultra-rare disease atypical hemolytic uremic syndrome (aHUS) and assigned it orphan drug status (4). Spurred by this success and recognizing the central role of complement in both common and rare diseases, large pharmaceutical companies, small start-ups, and academic laboratories have developed programs targeting different proteins in the complement cascade.

Many of these potentially new drugs are being studied in patients with C3 glomerulopathy (C3G), an ultra-rare kidney disease defined by underlying complement dysregulation and characterized by complement C3 deposition on kidney biopsy (5). Dysregulation of the alternative pathway (AP) is fundamental to disease expression, although terminal pathway dysregulation is also common. Treatment of C3G with eculizumab is unsuccessful in the majority of patients, consistent with the fact that eculizumab targets the terminal complement cascade and, therefore, primarily addresses only 1 aspect of C3G — glomerular inflammation — while leaving upstream C3 complement dysregulation untouched (6, 7).

Of upstream targets, factor D (FD), a 228–amino acid serine protease (SP) produced mainly by adipocytes, is appealing because it circulates in the plasma at very low concentrations and has a single function: to cleave its substrate, factor B (FB), in a $Mg^{2+}$-dependent complex with C3($H_2O$)B or C3bB in order to generate the C3 convertases of the AP, C3($H_2O$)Bb and C3bBb (8, 9). This role makes FD a key and rate-limiting component of the AP (10). Since the C3bBb amplification loop is integral to both the classical and lectin pathways, as well as the AP, the impact of FD inhibition is likely to be profound.

**Conflict of interest:** The authors have declared that no conflict of interest exists.



**Submitted:** December 18, 2019
**Accepted:** April 1, 2020
**Published:** May 7, 2020.

**Reference information:** *JCI Insight*. 2020;5(9):e135758. https://doi.org/10.1172/jci.insight.135758.

Mice with a targeted deletion of FH (*Cfh*$^{-/-}$) develop features of C3G and, on renal biopsy, show intense C3 deposition along glomerular capillary walls accompanied by subendothelial electron-dense deposits (11). To assess the impact of FD inhibition, we generated and studied complement activation in the *Cfh*$^{-/-}$ *Cfd*$^{-/-}$ mouse. We show that the C3G phenotype of the *Cfh*$^{-/-}$ mouse is not rescued by knocking out FD. Instead, the *Cfh*$^{-/-}$ *Cfd*$^{-/-}$ mouse develops a glomerular phenotype consistent with C3 glomerulonephritis (C3GN), a subtype of C3G, and nephrogenic diabetes insipidus (NDI). Serum from the *Cfh*$^{-/-}$ *Cfd*$^{-/-}$ mouse mediates small amounts of C3b deposition on sepharose, as well as hemolysis of rabbit erythrocytes, thereby revealing that residual AP function is present when both FD and FH are missing. Consistent with this observation, we show that C3($H_2O$), which is produced in the tick-over reaction (12, 13), directly increases hemolytic activity in vitro and in vivo and that inactivated C3($H_2O$) (iC3[$H_2O$]) is abundant in several tissues in the *Cfh*$^{-/-}$ *Cfd*$^{-/-}$ mouse, especially the kidney.

We propose that uncontrolled tick-over leads to the accumulation of C3($H_2O$), which — upon association with FB — is responsible for slow activation of the AP and the phenotype we observed in the *Cfh*$^{-/-}$ *Cfd*$^{-/-}$ mouse. When FD is absent, a minimal threshold of circulating FH is required if tissue deposition of C3 is to be prevented. When both FD and FH are present, the FD/FH ratio impacts serum C3 levels and renal C3 deposition. Importantly, in C3G patients with end-stage renal disease (ESRD), the FD/FH ratio is high; therefore, continuous and adequate AP control by targeting FD may be more difficult to achieve than expected.

## Results

*AP regulation in the fluid phase*. FD is the only known SP that cleaves FB bound to C3b (the C3 proconvertase, C3bB) to generate C3 convertase (C3bBb). Murine plasma from all 4 genotypes (*Cfh*$^{-/-}$, *Cfd*$^{-/-}$, *Cfh*$^{-/-}$ *Cfd*$^{-/-}$, and WT mice) was examined by ELISA and Western blotting to quantitate C3, FB, and C5. As reported by Pickering et al., C3 was depleted in *Cfh*$^{-/-}$ mice (11). In *Cfh*$^{-/-}$ *Cfd*$^{-/-}$ and WT mice, C3 levels were comparable, while in *Cfd*$^{-/-}$ mice, they were 40% higher. Western blotting showed C3α chains (a measure of C3) in all genotypes except *Cfh*$^{-/-}$ mice (Figure 1A). FB levels were significantly higher in *Cfh*$^{-/-}$ *Cfd*$^{-/-}$ mice as compared with WT mice ($P = 0.0073$). In addition to full-length FB (93 kDa), FB cleavage products were seen. Ba levels in WT mice reflect ongoing C3 tick-over. In *Cfh*$^{-/-}$ *Cfd*$^{-/-}$ mice, Ba levels were considerably lower than in WT mice, suggesting slower-than-normal C3 tick-over due to the absence of FD (Figure 1B). C5 levels were comparable across all genotypes, with the exception of *Cfh*$^{-/-}$ mice (Figure 1C). In aggregate, these results indicate that both AP fluid-phase and terminal pathway activity are under control in *Cfh*$^{-/-}$ *Cfd*$^{-/-}$ mice.

*AP dysregulation in the kidney*. *Cfh*$^{-/-}$ mice spontaneously develop C3G, with glomerular capillary C3 deposition evident very early in life (11). In *Cfh*$^{-/-}$ *Cfd*$^{-/-}$ mice, glomerular C3 and C5b-9 deposition were present in a mesangio-capillary distribution, consistent with ongoing complement activity in the kidney (Figure 2). The C3 glomerular distribution in *Cfh*$^{-/-}$ *Cfd*$^{-/-}$ mice differed from that seen in *Cfh*$^{-/-}$ and *Cfd*$^{-/-}$ mice (capillary and mesangial, respectively); however, within a given strain, C3c and C3d staining patterns were identical (Figure 2) (14). Glomerular C3 deposition was absent in 2-week-old *Cfh*$^{-/-}$ *Cfd*$^{-/-}$ mice but was seen by 1 month of age and increased thereafter (Figure 3A). Tubular C3 deposition started at 1 month and also increased with age (Figure 3B). Deposition of immunoglobulins was comparable with that seen in WT mice (Figure 3C). These findings show that local complement activity reflected by C3 and C5b-9 deposition is occurring in the kidneys of *Cfh*$^{-/-}$ *Cfd*$^{-/-}$ mice.

*Survival, proteinuria, and polyuria*. We monitored a group of *Cfh*$^{-/-}$ ($n = 24$), *Cfd*$^{-/-}$ ($n = 25$), *Cfh*$^{-/-}$ *Cfd*$^{-/-}$ ($n = 21$), and WT mice ($n = 12$) for 10 months. Mortality was significantly higher in *Cfh*$^{-/-}$ *Cfd*$^{-/-}$ mice as compared with *Cfh*$^{-/-}$ mice (> 50% versus < 10% at 10 months, respectively; $P < 0.0001$). There was no mortality in *Cfd*$^{-/-}$ and WT mice during this time period (Figure 4A). *Cfh*$^{-/-}$ *Cfd*$^{-/-}$ mice had elevated blood urea nitrogen (BUN) and serum creatinine at 8 months, with significant proteinuria (by strip test) and a urine albumin/creatinine ratio (UAC) approximately 2.5 times higher than in *Cfh*$^{-/-}$ mice (Figure 4, B and C). In *Cfd*$^{-/-}$ mice, the UAC was normal. Mild hematuria (trace to 1+) was present in 50% of *Cfh*$^{-/-}$ *Cfd*$^{-/-}$ 8-month-old mice. At 8 months, 24-hour urine volume was increased, reflecting progressive polyuria due to a decrease in urine concentrating ability (Figure 4, D–G). The polyuria did not respond to water deprivation or vasopressin (Table 1). C3 deposition was present in the proximal tubules of these animals (Figure 3B and Figure 4H). Thus *Cfh*$^{-/-}$ *Cfd*$^{-/-}$ mice have an increased mortality and also develop NDI.

*Histology*. Glomerular light microscopy revealed normal patterns in *Cfd*$^{-/-}$ mice at all ages (a representative 8-month-old mouse is shown in Figure 5A), while in *Cfh*$^{-/-}$ mice, mesangial and endocapillary hypercellularity were seen in older animals (8 months; Figure 5, B and C). In *Cfh*$^{-/-}$ *Cfd*$^{-/-}$ mice, glomeruli appeared relatively

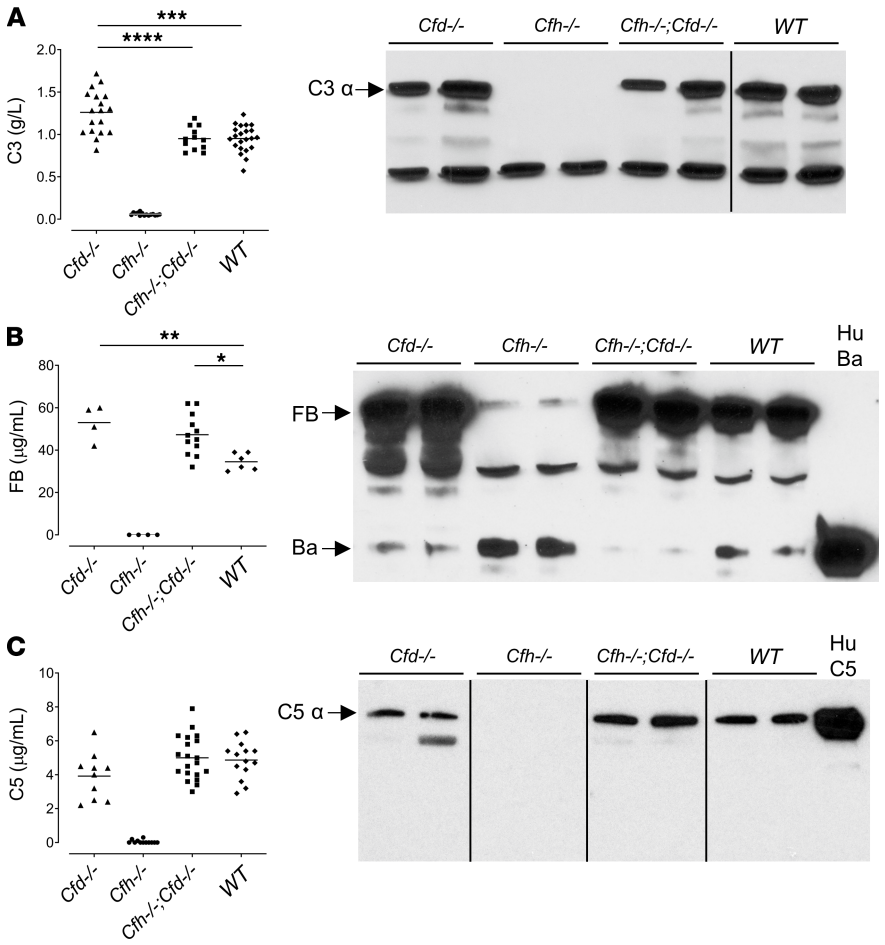


**Figure 1. Complement activity in the fluid phase.** (**A**) Plasma C3. C3 is depleted in *Cfh*$^{-/-}$ mice ($n$ = 15), while in *Cfh*$^{-/-}$ *Cfd*$^{-/-}$ ($n$ = 12) and WT mice ($n$ = 22), C3 levels are comparable. In *Cfd*$^{-/-}$ mice ($n$ = 18), C3 levels are 40% higher than in WT controls. Western blotting shows an intact C3 α chain in all genotypes except *Cfh*$^{-/-}$ mice. (**B**) Plasma FB. FB is significantly higher in *Cfh*$^{-/-}$ *Cfd*$^{-/-}$ ($n$ = 12) and *Cfd*$^{-/-}$ ($n$ = 4) mice as compared with WT controls ($n$ = 6), while FB is totally consumed in *Cfh*$^{-/-}$ mice ($n$ = 4). Its cleavage product, Ba, is seen in all genotypes on a Western blot, albeit at reduced levels in *Cfd*$^{-/-}$ and *Cfh*$^{-/-}$ *Cfd*$^{-/-}$ mice as compared with factor D–sufficient mice. Human Ba (Hu Ba) is shown as reference. (**C**) Plasma C5. C5 levels are comparable across all genotypes ($n$ = 10, 20, and 14 for *Cfd*$^{-/-}$, *Cfh*$^{-/-}$ *Cfd*$^{-/-}$, and WT mice, respectively), with the exception of *Cfh*$^{-/-}$ mice ($n$ = 12). On Western blotting, intact C5 α chains are present in all genotypes except for *Cfh*$^{-/-}$ mice. Human C5 (Hu C5) is shown as reference. Lines represent mean values. *$P$ < 0.05, **$P$ < 0.01,***$P$ < 0.001, ****$P$ < 0.0001 by 1-way ANOVA and Tukey post hoc test. Data from *Cfh*$^{-/-}$ were excluded in all statistical comparisons.

healthy at 2 months of age, with only moderate endocapillary hypercellularity; however, by 4 months of age, there was an increase in glomerular cellularity, an inflammatory infiltrate, and a thickening of the glomerular basement membrane (GBM) consistent with progressive GN (Figure 5, D–F and Table 2). Electron microscopy showed subendothelial and mesangial electron dense deposits (Figure 5, G–I; arrows). In aggregate, these findings, together with the C3 immunofluorescence, confirm the diagnosis of C3GN.

*In vitro complement activity*. We used a C3b deposition assay to evaluate complement activation. In WT mice, Sepharose 4B activates complement through the AP in buffer containing EGTA and $Mg^{2+}$ (15). As expected, activation was not possible in *Cfh*$^{-/-}$ mice, as several complement proteins (C3, FB, and C5) are depleted. No C3b deposition was observed in *Cfd*$^{-/-}$ mice; however, upon the addition of human FD, C3b deposition was restored. In *Cfh*$^{-/-}$ *Cfd*$^{-/-}$ mice, low levels of C3b deposition were detectable (~20% as compared with WT mice). The addition of human FH to sera from *Cfh*$^{-/-}$ *Cfd*$^{-/-}$ mice prevented this deposition, while the addition of human FD had no effect (Figure 6A). A rabbit erythrocyte hemolytic assay was used to confirm complement activity in *Cfh*$^{-/-}$ *Cfd*$^{-/-}$ mice and documented variable low levels of hemolysis (30%–70%) in the presence of EGTA and $Mg^{2+}$ that were preventable by the addition of human FH (Figure 6B), soluble CR1, and BB5.1, a mouse C5 antibody that inhibits the terminal pathway (results not shown) (16).

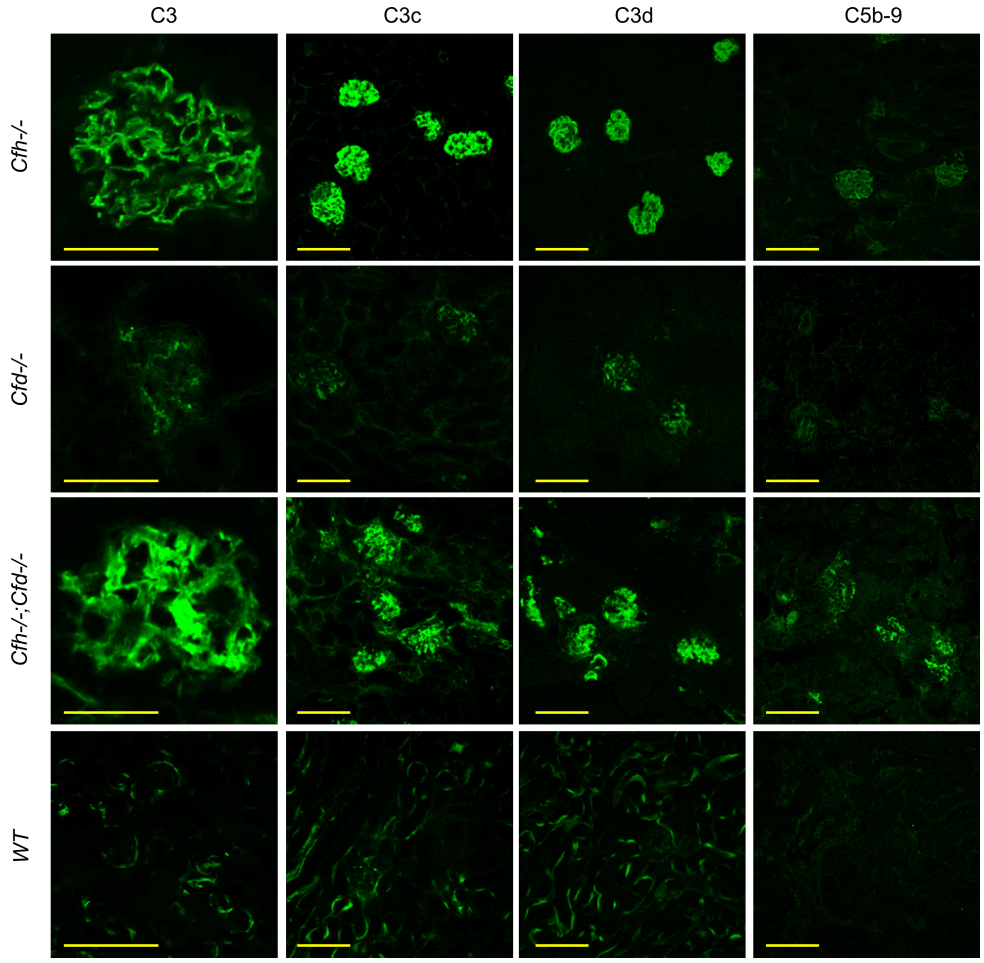


**Figure 2. Complement activity in the kidney.** Complement dysregulation in the kidney as reflected in glomerular immunofluorescence staining for C3, C3c, and C3d (as a reflection of AP activity), as well as C5b-9 (as a reflection of terminal pathway activity) on frozen renal sections from 8-month-old *Cfh*$^{-/-}$, *Cfd*$^{-/-}$, *Cfh*$^{-/-}$ *Cfd*$^{-/-}$, and WT mice. Scale bars: 50 μM for C3 staining; 100 μM for C3c, C3d, and C5b-9 staining.

Plasma kallikrein (PK) is a SP that is responsible for the release of bradykinin from high molecular–weight kininogen (17). It has been reported to cleave FB bound to C3b in vitro (18, 19). While we confirmed this activity and validated the cutting site (PK cuts FB bound to C3b at the same site as FD), PK-mediated cleavage was very slow (half-life, 10 minutes) and was > 25 times less efficient than FD-mediated cleavage, consistent with other reports (Supplemental Figure 1; supplemental material available online with this article; https://doi.org/10.1172/jci.insight.135758DS1) (18). The amount of hemolysis induced by sera from *Cfh*$^{-/-}$ *Cfd*$^{-/-}$ mice did not change when the rabbit erythrocyte hemolytic assay was supplemented with PK or when a PK inhibitor (PKSI-527) was added (Figure 6C, red line). PKSI-527 introduced to *Cfh*$^{-/-}$ *Cfd*$^{-/-}$ mice by i.p. injection failed to alter glomerular C3 deposition as compared with PBS-injected littermate controls (results not shown). These findings imply that low-level C3 activation is occurring in *Cfh*$^{-/-}$ *Cfd*$^{-/-}$ mice but that PK is not cleaving C3($H_2O$)B. We also excluded the involvement of MASP-3, C1s, FVIIa, FIXa, FXa, FXIa, FXIIa, FXIIIa, thrombin, plasmin, and activated protein C (APC) using the same in vitro FB cleavage assay. APC and plasmin cut C3b-bound FB but at cutting rates even slower than rates mediated by PK (results not shown).

While conducting the above experiments, we found high concentrations (> 200 μg/mL) of human C1-inhibitor (C1-Inh) could suppress hemolysis induced by sera from *Cfh*$^{-/-}$ *Cfd*$^{-/-}$ mice (Figure 6C, blue line) through a PK-independent mechanism. This effect was confirmed by infusion of Berinert, a medicinal grade C1-Inh, into *Cfh*$^{-/-}$ *Cfd*$^{-/-}$ mice. Sera taken from mice that received the infusion could not promote hemolysis of rabbit erythrocytes (results not shown). These data are consistent with the reported C1-Inh

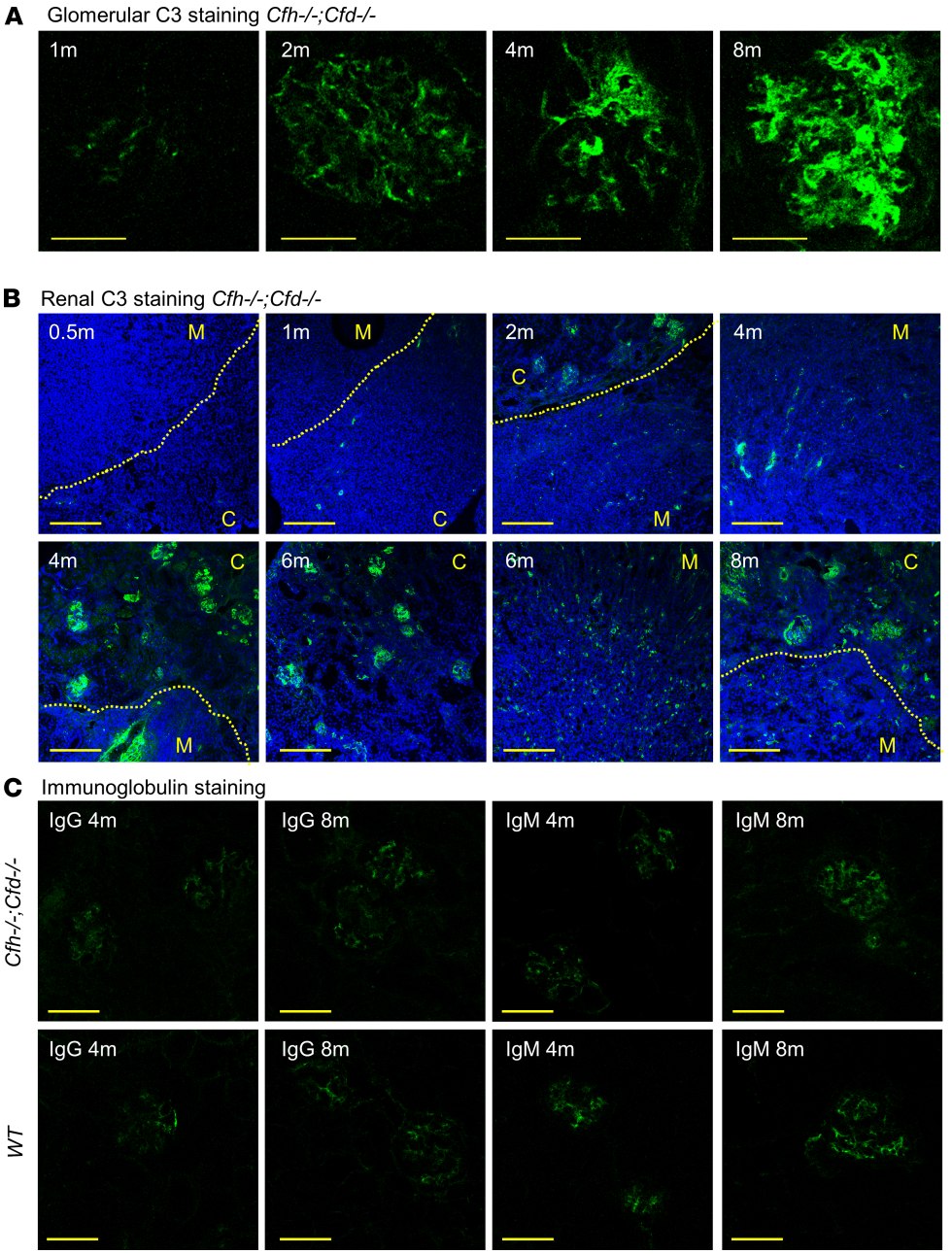


**Figure 3. Longitudinal studies of renal C3 and immunoglobin depositions.** (**A**) Glomerular C3 accumulates over time in *Cfh*$^{-/-}$ *Cfd*$^{-/-}$ mice and concentrates in the mesangium. Scale bars: 50 μM. (**B**) Renal C3 immunofluorescence increases over time in *Cfh*$^{-/-}$ *Cfd*$^{-/-}$ mice ranging in age from 0.5–8 months. Tubular C3 staining gradually spreads from cortex to medulla. The yellow lines trace the boundary of renal cortex (C) and renal medulla (M); blue, DAPI. Scale bars: 200 μM. (**C**) Glomerular immunoglobulin deposition in *Cfh*$^{-/-}$ *Cfd*$^{-/-}$ and WT mice. Deposition of IgG and IgM at both 4 and 8 months in *Cfh*$^{-/-}$ *Cfd*$^{-/-}$ mice is comparable with deposition seen in WT controls. Scale bars: 100 μM.

function on the AP (20). Jiang et al. have shown that, in marked molar excess, C1-Inh binds to C3b (but not FB) and reduces AP activity. Therefore, we hypothesized that, because tick-over is not controlled in *Cfh*$^{-/-}$ *Cfd*$^{-/-}$ mice, a substantial amount of circulating C3 is transformed into C3($H_2O$), which is responsible for low-grade hemolysis. Adding either FH or C1-Inh blocks the interaction between C3($H_2O$) and FB, thereby preventing hemolysis.

*C3($H_2O$), tick-over, and glomerular iC3($H_2O$) deposition*. The spontaneous hydrolysis of C3 occurs in a process known as tick-over. Methylamine-treated C3 (C3[MA]) mimics the structure of C3($H_2O$) (21). To test whether C3($H_2O$) could be responsible for the unusual hemolytic activity in *Cfh*$^{-/-}$ *Cfd*$^{-/-}$ mice, we supplemented sera

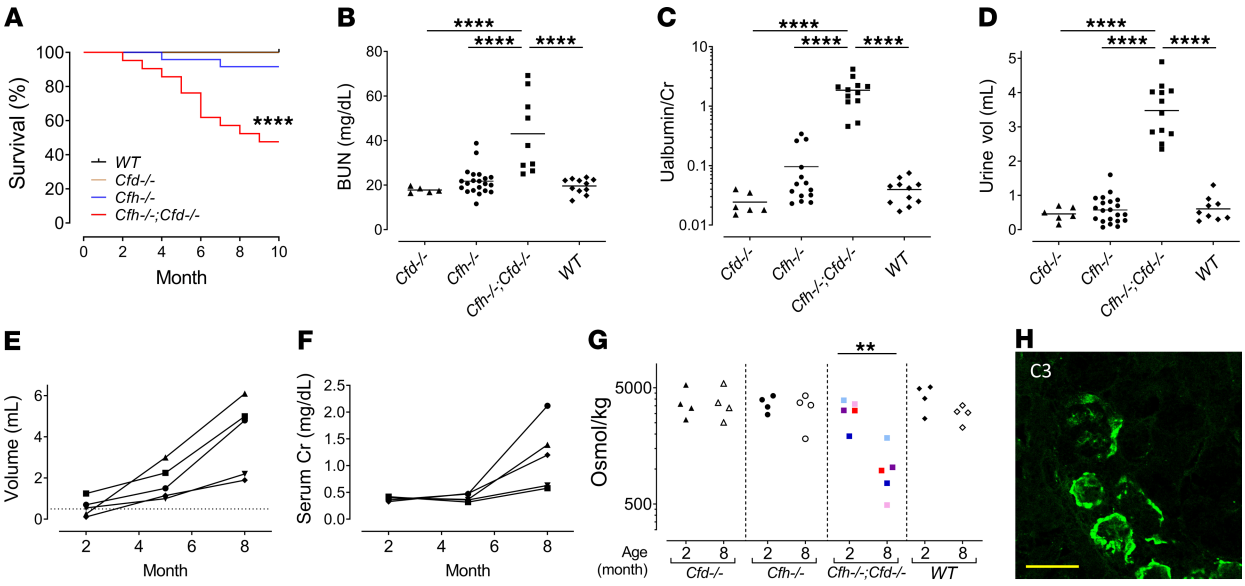


**Figure 4. Survival and renal function.** (**A**) Survival curve. *Cfd*$^{-/-}$ (bronze line, $n$ = 25) and WT (black dot, $n$ = 12) mice have similar survival as compared with the > 50% 10-month mortality of *Cfh*$^{-/-}$ *Cfd*$^{-/-}$ mice (red line, $n$ = 21) and the 10% 10-month mortality of *Cfh*$^{-/-}$ mice (blue line, $n$ = 24); ****$P$ < 0.0001 (*Cfh*$^{-/-}$ *Cfd*$^{-/-}$ versus 3 groups) by Mantel-Cox logrank test. (**B** and **C**) BUN and urine albumin/creatinine ratio at 8 months are significantly elevated in *Cfh*$^{-/-}$ *Cfd*$^{-/-}$ mice (line represents mean). (**D**) Polyuria. Urine volume (24-hour) is significantly increased in aged *Cfh*$^{-/-}$ *Cfd*$^{-/-}$ mice (age for all genotypes, 8 months). (**E** and **F**) In *Cfh*$^{-/-}$ *Cfd*$^{-/-}$ mice ($n$ = 5), polyuria and serum creatinine (serum Cr) increase with age, with each line representing disease progression in an individual mouse (dashed line in **E** represents average 24-urine output in WT animals). (**G**) Urine osmolarity decreases in aged *Cfh*$^{-/-}$ *Cfd*$^{-/-}$ mice (8-month) but not in young mice (2-month) or other genotypes, with each color representing the same *Cfh*$^{-/-}$ *Cfd*$^{-/-}$ mouse. (**H**) Tubular staining for C3 in the kidney of *Cfh*$^{-/-}$ *Cfd*$^{-/-}$ mice. Scale bar: 50 μM. For **B**, **C**, **D**, and **G**, each symbol represents 1 datum for an animal. ****$P$ < 0.0001 by 1-way ANOVA and Tukey post hoc test for **B**, **C**, and **D**. **$P$ < 0.01 by 2-tailed paired $t$ test for **G**.

from *Cfh*$^{-/-}$ *Cfd*$^{-/-}$ mice with either C3(MA) or C3 in the rabbit erythrocyte hemolytic assay. We observed an increase in hemolysis of 10%–20% with C3(MA) but no change with C3 (Figure 6D). We then injected human C3 or C3(MA) into *Cfh*$^{-/-}$ *Cfd*$^{-/-}$ mice. Both hemolytic activity and glomerular C3 deposition increased in C3(MA)-injected but not in C3-injected mice, implying that C3($H_2O$) induces the observed complement activity (Figure 6, E and F). While C3($H_2O$) or iC3($H_2O$) is present in the plasma of *Cfh*$^{-/-}$ *Cfd*$^{-/-}$ mice at low concentrations, both are present in the kidney (Figure 6G). The amount of renal iC3($H_2O$) increases as animals age and is most abundant in the kidney, as compared with levels in other organs like the liver, spleen, heart, and eye (Supplemental Figure 2).

*Human FH restores complement regulation in vivo in Cfh*$^{-/-}$ *Cfd*$^{-/-}$ *mice*. Because *Cfh*$^{-/-}$ *Cfd*$^{-/-}$ mice lack both FH and FD, we sought to determine the impact of incremental factor replacement (Figure 7, A and B). Supplementation with human FH corrected C3 deposition and abnormal hemolysis in sera from *Cfh*$^{-/-}$ *Cfd*$^{-/-}$ mice. To determine the minimum concentration of FH required to control (C3[$H_2O$])B-mediated tick-over in vivo, we injected human FH i.p. in *Cfh*$^{-/-}$ *Cfd*$^{-/-}$ mice. C3 deposition was still detectable when plasma FH concentrations were 20 μg/mL (with a dose of 5 mg/kg) but was substantially reduced at concentrations greater than 50 μg/mL (with a dose of 20 mg/kg) (Figure 7A). Thus, without FD, the minimal plasma concentration of human FH required to control the tick-over–associated renal damage in *Cfh*$^{-/-}$ *Cfd*$^{-/-}$ mice was approximately 50 μg/mL or 25% of normal FH levels.

*Human FD activates complement in vivo in Cfh*$^{-/-}$ *Cfd*$^{-/-}$ *mice*. FD circulates at very low concentrations (1–2 μg/mL) and is the rate-limiting enzyme in the activation of the AP (10). To determine the minimum amount of FD required to activate the AP in the absence of FH, we injected human FD i.p. in *Cfh*$^{-/-}$ *Cfd*$^{-/-}$ mice and observed that very small doses of FD (0.1 μg/kg or 2 ng for 20 g mice, equivalent to 0.1% of total FD in WT mouse) resulted in a 50% drop in plasma C3 levels (Figure 7, B and C), simultaneously changing the pattern of C3 glomerular deposition to that seen in *Cfh*$^{-/-}$ mice (Figure 7B). A single FD dose of 1 μg/kg resulted in complete C3 depletion by 4–6 hours after injection, with levels fully recovering by 24 hours (Figure 7D). Injected FD is undetectable in the circulation, even with the highest dose (250 μg/kg), consistent with its high metabolic rate and possible loss through the renal glomerulus.

**Table 1. Water deprivation study**

| | 24 hours with water | | | 9 hours without water | | | 3 hours after ADH i.p. | | |
|---|---|---|---|---|---|---|---|---|---|
| Age | *Cfh*$^{-/-}$ *Cfd*$^{-/-}$ | *Cfh*$^{-/-}$ | *Cfd*$^{-/-}$ | *Cfh*$^{-/-}$ *Cfd*$^{-/-}$ | *Cfh*$^{-/-}$ | *Cfd*$^{-/-}$ | *Cfh*$^{-/-}$ *Cfd*$^{-/-}$ | *Cfh*$^{-/-}$ | *Cfd*$^{-/-}$ |
| 4-month-old | | | | | | | | | |
| No. of mice, urine > 100 μL | 4 | 2 | 4 | 0 | 0 | 0 | 0 | 0 | 0 |
| No. of mice, urine < 100 μL | 0 | 0 | 0 | 4 | 2 | 4 | 4 | 2 | 4 |
| 8-month-old | | | | | | | | | |
| No. of mice, urine > 100 μL | 5 | 2 | 4 | 5 | 0 | 1 | 5 | 0 | 0 |
| No. of mice, urine < 100 μL | 0 | 0 | 0 | 0 | 2 | 3 | 0 | 2 | 4 |

ADH, antidiuretic hormone.

*Interaction between FH and FD and levels of FD in renal disease*. C3 is consumed when FH is absent (*Cfh*$^{-/-}$ mice), but when both FH and FD are missing (*Cfh*$^{-/-}$ *Cfd*$^{-/-}$ mice), C3 levels are restored. I.p. injections of varying concentrations of FH in the presence of a constant dose of FD (1 μg/kg) showed that the minimum concentration of FH required to control AP activity in the fluid phase is about 30 μg/mL (Figure 7E). Plasma C3 is inversely correlated with the FD/FH ratio (Figure 7F). However, when the dose of FD was increased to 100 μg/kg, the same concentration of FH failed to normalize plasma C3 (Figure 7G).

*FH and FD in patients with C3G*. High Ba is associated with ESRD and strictly correlates with creatinine clearance (22). FD is highly elevated in patients with ESRD, while FH is not (Figure 8, A and B), significantly increasing FD/FH ratios in these patients (Figure 8C). In C3G patients with elevated levels of FD (> 3 μg/mL; normal < 2 μg/mL) and without detectable autoantibodies (to mimic conditions in the *Cfh*$^{-/-}$ *Cfd*$^{-/-}$ mouse), we found that the FD/FH ratio correlated weakly with plasma C3 levels ($P = 0.042$, Figure 8D) but strongly with plasma C5 levels ($P = 0.0002$, Figure 8E). Thus, higher levels of FD are associated with lower complement control for a given level of FH in C3G patients with ESRD. The FD/FH ratio is important in establishing control of the AP and may impact the efficacy of FD-targeted complement inhibition if constant and complete FD inhibition is not achieved.

## Discussion

Uncontrolled AP activation in the *Cfh*$^{-/-}$ mouse leads to consumption of serum C3 and its concomitant deposition in the renal glomerulus (11). Since FD cleaves FB to activate the C3 convertase, we hypothesized that this uncontrolled complement activity could be corrected in the *Cfh*$^{-/-}$ mouse by deleting FD and that the renal phenotype would be rescued. To our surprise, the *Cfh*$^{-/-}$ *Cfd*$^{-/-}$ mouse developed a more severe C3G phenotype. Over 50% of *Cfh*$^{-/-}$ *Cfd*$^{-/-}$ mice die by 10 months of age as a result of progressive crescentic GN (Figures 4A and Figure 5). In addition, all animals develop NDI between 5 and 10 months of age due to tubular damage associated with C3 deposition (Figure 3B and Figure 4).

*Cfh*$^{-/-}$ *Cfd*$^{-/-}$ and WT mice have comparable levels of circulating C3, indicating that, in the fluid phase, the amplification loop of the AP is abolished by removal of FD (Figure 1A). However, small amounts of Ba, a cleavage product of FB, are identifiable in the plasma of *Cfh*$^{-/-}$ *Cfd*$^{-/-}$ mice, providing indirect evidence for some complement activation. Residual but low AP activity was also confirmed by both sepharose C3b deposition and rabbit erythrocyte hemolytic assays (Figure 6, A and B).

Consistent with the presence of low AP activity, glomerular and tubulointerstitial C3 staining is seen in *Cfh*$^{-/-}$ *Cfd*$^{-/-}$ mice (Figure 2 and Figure 3). The glomerular C3 staining is identifiable in 1-month-old *Cfh*$^{-/-}$ *Cfd*$^{-/-}$ mice in a pattern that is mostly mesangial but progresses with age to become mesangial and capillary (Figure 3A). *Cfh*$^{-/-}$ mice, by comparison, show prominent and constant glomerular capillary C3 deposition throughout life (11). These differences in C3 deposition reflect, at least in part, the kinetics of C3 turnover. *Cfh*$^{-/-}$ mice lack FH, the primary regulator of complement; therefore, C3bBb convertase activity is unchecked, C3 is consumed (circulating C3 is close to zero), and large amounts of C3b degradation products deposit on glomerular endothelial and mesangial cells. In *Cfh*$^{-/-}$ *Cfd*$^{-/-}$ mice, C3 serum levels are normal, but C3($H_2O$), which is abundant due to the absence of both FH and FD, slowly and continuously deposits in the glomeruli (Figure 3A). Tubulointerstitial C3 staining is also seen in *Cfh*$^{-/-}$ *Cfd*$^{-/-}$ (Figure 3B). It differs from the linear tubulointerstitial C3 staining present in WT mice, which reflects normal local complement activity (Figure 2, bottom row) (23, 24). In *Cfh*$^{-/-}$ *Cfd*$^{-/-}$ mice, the source is C3($H_2O$), and the staining pattern is intense with bumps and humps (Figure 3B).

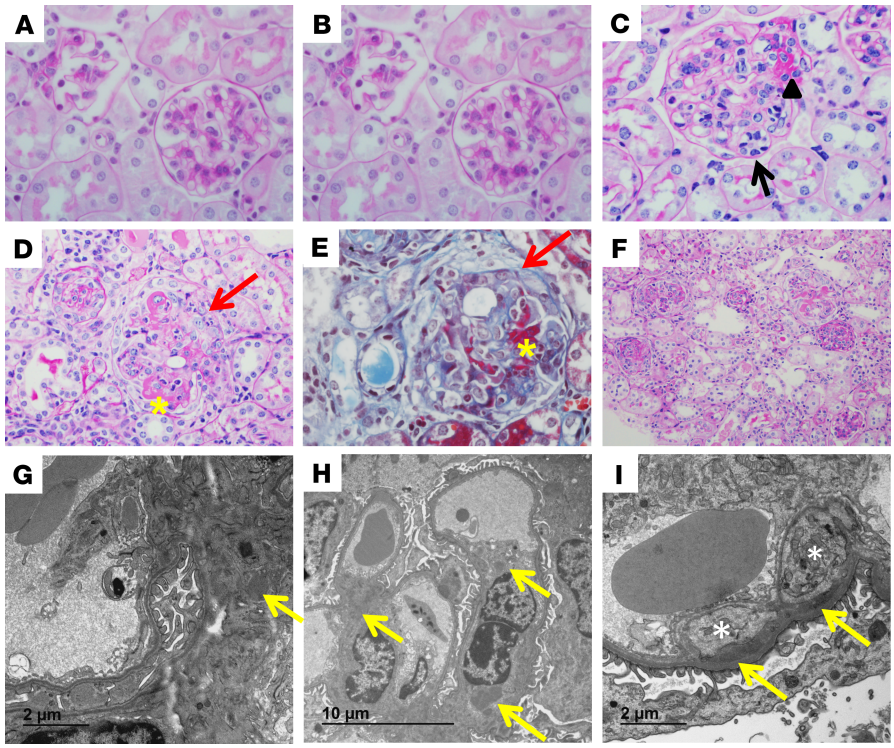


**Figure 5. Kidney histology.** (**A**) Normal glomeruli in *Cfd*$^{-/-}$ mice (age, 8 months). (**B**) Mesangial hypercellularity in *Cfh*$^{-/-}$ mice (age, 8 months). (**C**) Endocapillary hypercellularity (arrow) and segmental sclerosis (arrowhead) in *Cfh*$^{-/-}$ mice (age, 8 months). (**D** and **E**) Segmental necrosis (asterisk) and crescents (red arrow) in *Cfh*$^{-/-}$ *Cfd*$^{-/-}$ mice (age, 4 months). (**F**) By 8 months, diffuse necrotizing and crescentic glomerulonephritis involves the majority of glomeruli in *Cfh*$^{-/-}$ *Cfd*$^{-/-}$ mice. (**G**, **H**, and **I**) Electron microscopy in 3 *Cfh*$^{-/-}$ *Cfd*$^{-/-}$ mice shows mesangial (arrows in **G** and **H**) and subendothelial deposits (arrows in **I**). Total magnification, 60× (**A**–**E**) 20× (**F**). **A**–**D** and **F** show PAS staining; **E** shows Masson trichrome staining.

Why does C3($H_2O$) accumulate in *Cfh*$^{-/-}$ *Cfd*$^{-/-}$ mice? AP initiation, or tick-over, refers to the spontaneous hydrolysis of C3 that occurs at a slow and constant rate of about 0.2%–0.4% per hour (12). With hydrolysis, C3 undergoes a major conformation change that exposes the thiol ester bond, which can react with adjacent hydroxyl (-OH) and amine (-NH2) groups either on nearby circulating proteins or on cell surfaces (25, 26). In WT or *Cfd*$^{-/-}$ mice, both of which are sufficient in FH, C3($H_2O$) has an extremely short half-life, and only small amounts of C3($H_2O$) (<5%) can bind covalently to surfaces (26). Thus, the impact of C3($H_2O$) is neutralized by FH, which blocks FB binding and facilitates factor I-mediated cleavage to generate iC3($H_2O$), albeit at a much slower rate than the corresponding cleavage of C3b to iC3b (12).

In *Cfh*$^{-/-}$ *Cfd*$^{-/-}$ mice, the continuously generated C3($H_2O$) accumulates in the serum in the absence of FH and serves as a continual source for C3 deposition on cell surfaces. Once surface bound, C3($H_2O$) can associate with FB to form C3($H_2O$)B or undergo cleavage by factor I in the presence of cofactors such as Crry to iC3($H_2O$). iC3($H_2O$), which cannot form new fluid-phase convertases, induces local inflammatory cytokine production by binding to complement receptor 3 (CR3) and is abundantly present in the kidneys of *Cfh*$^{-/-}$ *Cfd*$^{-/-}$ mice over 5 months of age (Figure 6G) (27).

We did not initially consider C3($H_2O$)B as the source of low-level AP activity and instead considered possible bypass convertases. We studied and excluded the involvement of MASP-3, C1s, FVIIa, FIXa, FXa, FXIa, FXIIa, FXIIIa, thrombin, plasmin, and APC using an in vitro FB cleavage assay. We also tested PK, a SP known to cleave C3b-bound FB in vitro (18). We confirmed this activity but noted the cutting rate was very slow and that addition of either PK or a PK inhibitor to the sepharose C3b deposition or rabbit erythrocyte hemolytic assays did not alter the kinetics in these experiments (Supplemental Figure 1). Furthermore, i.p. injection of PK or a PK inhibitor in *Cfh*$^{-/-}$ *Cfd*$^{-/-}$ mice had no observable impact on renal C3 deposition. These experiments made it unlikely that a bypass mechanism was driving the disease process.

While conducting the above experiments, we discovered that high concentrations of human C1-Inh suppressed hemolysis induced by sera from *Cfh*$^{-/-}$ *Cfd*$^{-/-}$ mice through a PK-independent mechanism

**Table 2. Renal pathology score**

| Genotype | Severity | | | | |
|---|---|---|---|---|---|
| | Normal | Mesangial | Endocapillary | Seg Scl | Cres/SN |
| WT | 94% | 6% | | | |
| WT | 95% | 5% | | | |
| WT | 95% | 5% | | | |
| *Cfd*$^{-/-}$ | 97% | 3% | | | |
| *Cfd*$^{-/-}$ | 99% | 1% | | | |
| *Cfd*$^{-/-}$ | 97% | 3% | | | |
| *Cfh*$^{-/-}$ | 70% | 28% | 2% | 1% | |
| *Cfh*$^{-/-}$ | 65% | 21% | 7% | 8% | |
| *Cfh*$^{-/-}$ | 46% | 47% | 4% | 3% | |
| *Cfh*$^{-/-}$ *Cfd*$^{-/-}$ | 17% | 5% | 3% | 22% | 52% |
| *Cfh*$^{-/-}$ *Cfd*$^{-/-}$ | 40% | 14% | 12% | 14% | 20% |
| *Cfh*$^{-/-}$ *Cfd*$^{-/-}$ | 4% | 2% | 26% | 33% | 36% |

At least 100 glomeruli (PAS stained slices from 3 mice ($n$ = 3) of each genotype) were scored. Seg Scl, segmental sclerosis/fibrous crescent; Cres/SN, cellular crescents/segmental necrosis

(Figure 6C, blue line) suggesting that C3($H_2O$) was responsible for the unchecked AP activity. Both C3($H_2O$) and C3b associate with FB to form convertases. Once C3($H_2O$)B and C3bB have formed, cleavage of the FB scissile bond by FD yields the central protease complexes (C3[$H_2O$]Bb and C3bBb) that amplify the complement response. In *Cfd*$^{-/-}$ and *Cfh*$^{-/-}$ *Cfd*$^{-/-}$ mice (FD deficient), FB is significantly elevated (Figure 1B), reflecting lower consumption of FB. In the presence of $Mg^{2+}$, FB in the C3 pro-convertase (C3[$H_2O$]B) engages in 2 conformation switches, "closed" and "open" (28). In the closed state, the scissile bond is not accessible, while in the open state, uncut but bound FB exhibits low enzymatic activity. Our data show that C3($H_2O$)B$^{open}$ acts as a weak C3 convertase on cell surfaces. In the kidney, for example, it cleaves C3 to C3b, eventually leading to activation of the terminal pathway (Figure 2, C5b-9 staining).

The *Cfh*$^{-/-}$ *Cfd*$^{-/-}$ mouse also allowed us to study the consequence of restoring either FD or FH by i.p. injection. We found the impact of FD to be profound even in small amounts. For example, injecting *Cfh*$^{-/-}$ *Cfd*$^{-/-}$ mice with a miniscule amount of human FD estimated at 0.1% of WT FD levels dropped C3 levels by 50% within a few hours (Figure 7C). Using FH, we found that the minimal concentration required to control tick-over was about 50 μg/mL or 25% of normal FH levels. When the concentration of FH was varied in the presence of a constant dose of FD (1 μg/kg), we could show that plasma C3 inversely correlated with the FD/FH ratio (Figure 7F) and that at least 30 μg/mL of FH was required to control AP activity in the fluid phase. This same dose of FH, however, failed to normalize plasma C3 if the dose of FD was increased (Figure 7G).

These findings are of clinical relevance to patients with C3G, despite the fact that combined deficiency of both FD and FH has not been seen. Deficiency of either FD or FH, however, has been reported, albeit rarely. The former has been identified in patients from 4 families who presented with a nonfunctional AP, making them prone to Neisserial infections (29–32). They were otherwise normal. The latter has been seen in at least 12 families and has been implicated in both GN (membranoproliferative glomerulonephritis type I or C3G; 9 families) and aHUS (33–39).

As compared with complete deficiency, partial deficiency of FH is much more common and is typically seen in C3G patients in association with genetic mutations or FH autoantibodies that render FH functionally deficient (5, 40). As renal function deteriorates in these patients, FD levels increase and can rise, in some cases, to > 20-fold above normal (Figure 8A) (41). In C3G patients with ESRD who are negative for nephritic factors, we observed a direct association between complement activity and FD levels, as reflected by C3 and C5 levels. Although C3 levels were weakly correlated with the FD/FH ratio, the correlation between C5 levels and the FD/FH ratio was very strong. This difference may reflect the higher catabolic rate of C3, which has a turnover rate that is about 10 times higher than the rate for C5 (C3, 2%/hour; C5, 0.2%/hour) (42, 43).

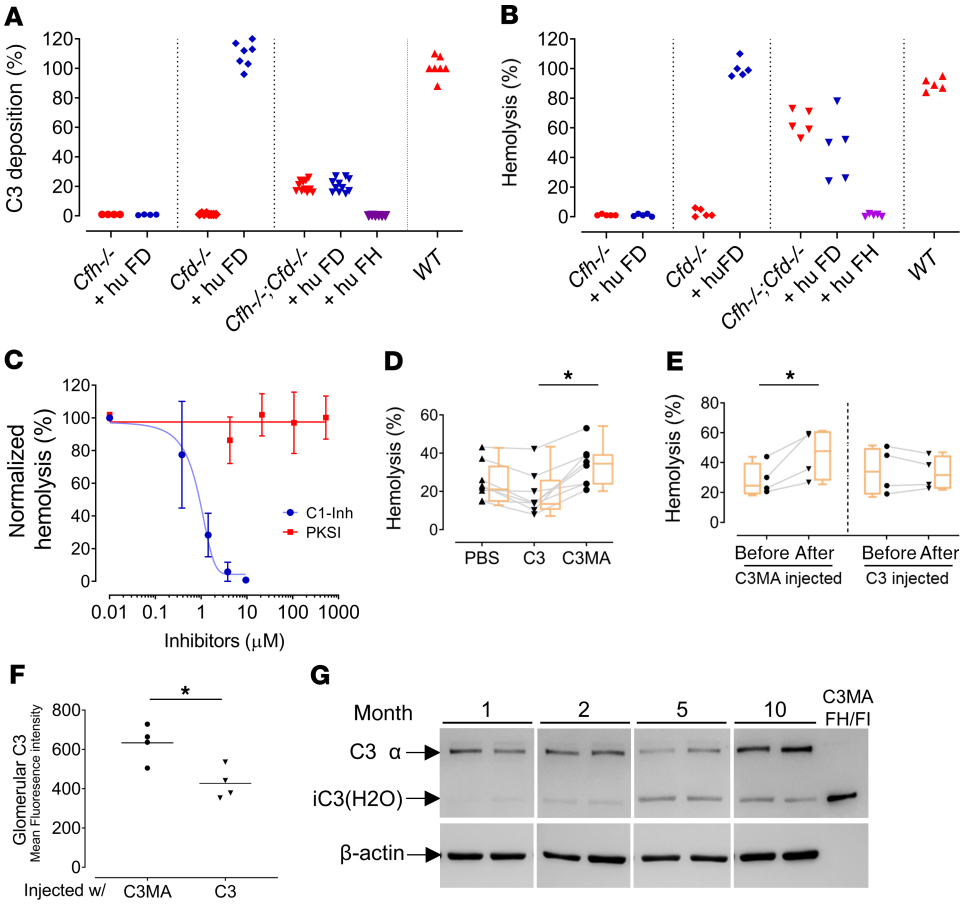


**Figure 6. Mechanism of action underlying complement activation in the absence of FH and FD.** (**A**) Sepharose C3b deposition (SC3D) assay. No SC3D is observed using serum from *Cfh*$^{-/-}$ ($n$ = 4) or *Cfd*$^{-/-}$ ($n$ = 7) mice; however, C3b deposition is restored when human FD (huFD) is added to the serum of *Cfd*$^{-/-}$ but not *Cfh*$^{-/-}$ mice. A small amount of C3b deposition is detectable using serum from *Cfh*$^{-/-}$ *Cfd*$^{-/-}$ mice ($n$ = 11); addition of huFD does not improve the deposition, while addition of huFH quenches it. Serum collected for WT mice ($n$ = 7) is used as a control. (**B**) Hemolytic assay using rabbit erythrocytes (RaE). Consistent with the SC3D results, there are moderate levels of hemolysis using serum from *Cfh*$^{-/-}$ *Cfd*$^{-/-}$ mice. The addition of huFD does not alter the hemolysis, while the addition of huFH suppresses it. Data in each group are derived from serum collected from 5 individual mice. (**C**) Addition of C1-Inh at high concentrations to *Cfh*$^{-/-}$ *Cfd*$^{-/-}$ serum ($n$ = 6, mean ± SD) prevents residual hemolysis, while addition of the plasma kallikrein inhibitor PKSI-527 ($n$ = 4) has no effect, consistent with C3($H_2O$)-associated residual AP activity in the serum of *Cfh*$^{-/-}$ *Cfd*$^{-/-}$ mice. (**D**) Addition of human C3(MA) to *Cfh*$^{-/-}$ *Cfd*$^{-/-}$ serum increases hemolysis of RaE, but the addition of C3 does not ($n$ = 5, mean values are used in box plots). (**E**) Injection of C3(MA) in *Cfh*$^{-/-}$ *Cfd*$^{-/-}$ mice increases subsequent serum-mediated ex vivo hemolysis of RaE, while injection of C3 does not increase hemolysis ($n$ = 4 for both groups). (**F**) Glomerular C3 deposition is also increased with the injection of C3(MA) ($n$ = 4) compared with deposition with C3 injection ($n$ = 4). (**G**) Local iC3($H_2O$) deposition over time. Supernatants from homogenized kidney tissues of *Cfh*$^{-/-}$ *Cfd*$^{-/-}$ mice ($n$ = 2 for each age group) show increased iC3($H_2O$) with age as resolved on a Western blot probed with an anti-C3a antibody (β-actin, loading control). *$P$ < 0.05 by 2-tailed paired $t$ test for **D** and **E** or unpaired 2-tailed $t$ test for **F**.

In summary, the *Cfh*$^{-/-}$ *Cfd*$^{-/-}$ mouse has provided valuable insights into our understanding of complement activation. We show that C3($H_2O$)B$^{open}$ is a weak C3 convertase, which can nevertheless lead to severe renal disease, and that very small amounts of FD are sufficient to activate complement. These findings suggest that efforts to block AP activity by targeting FD may lead to unanticipated outcomes in subgroups of C3G patients. In those rare patients with complete FH deficiency, we would expect the renal phenotype to be aggravated by FD-targeted treatment, and in patients with ESRD and partial-to-severe FH deficiency, as FD levels increase with declining renal function, sustained complete and persistent FD blockade may be difficult to maintain, with breakthrough complement activation occurring as even miniscule amounts of free FD become available.

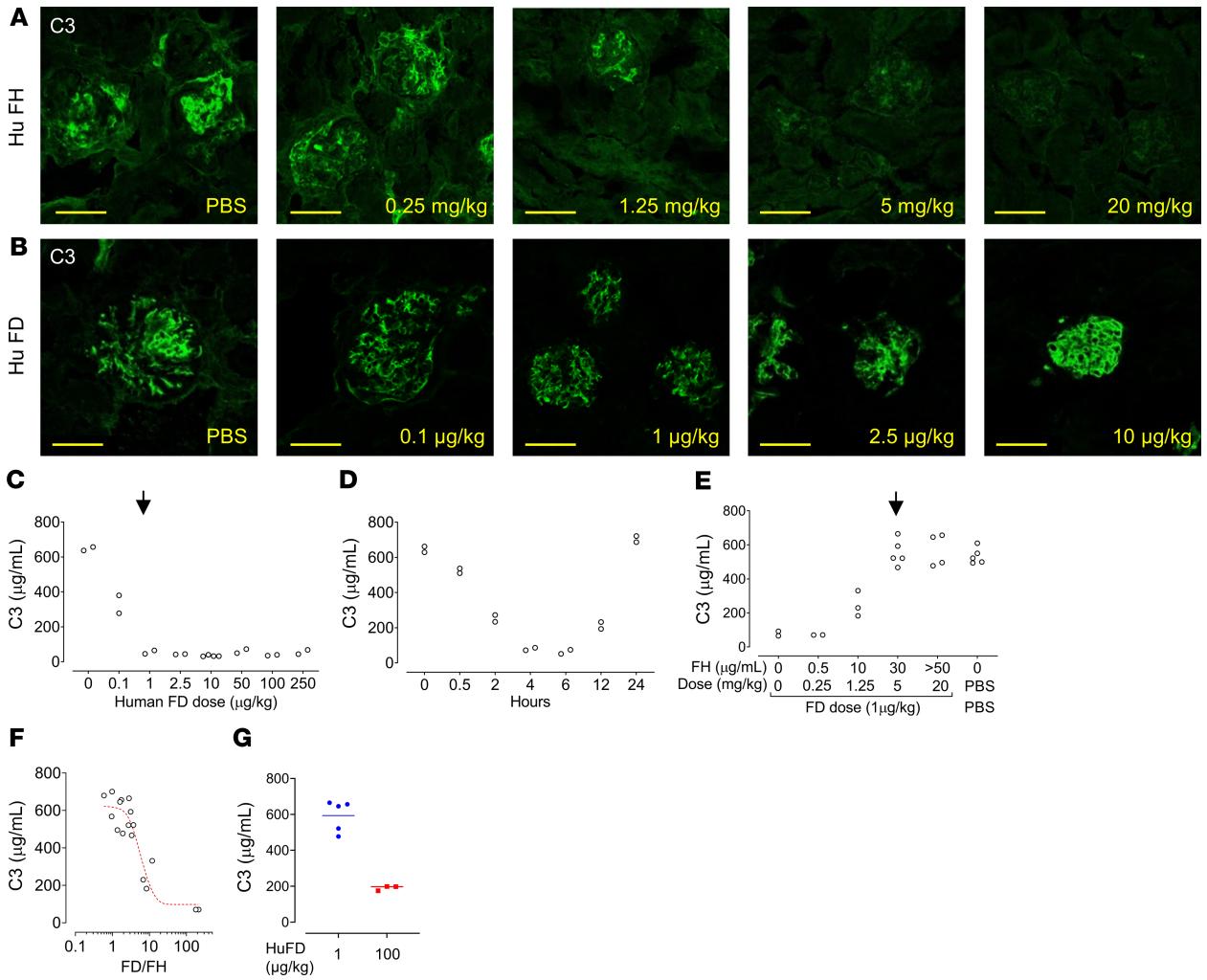


**Figure 7. FH and FD modulate renal C3 deposition in *Cfh*$^{-/-}$ *Cfd*$^{-/-}$ mice.** (**A**) Injection of human FH decreases and eventually eliminates C3 deposition in *Cfh*$^{-/-}$ *Cfd*$^{-/-}$ mice in a dose-dependent manner. (**B**) The C3 deposition pattern changes from predominantly mesangial to capillary, with increasing amounts of human FD (from left to right). For **A** and **B**, each image represents 3 injected mice with 10 glomeruli surveyed under each condition. Scale bars: 50 μM. (**C** and **D**) Pharmacodynamics of human FD in *Cfh*$^{-/-}$ *Cfd*$^{-/-}$ mice. The minimum concentration of FD required to deplete complement (arrow, **C**) and the time-to-deplete and time-to-restore C3 after a single dose of human FD (1 μg/kg, **D**). (**E**) Pharmacodynamics of human FH and FD in *Cfh*$^{-/-}$ *Cfd*$^{-/-}$ mice. C3 levels in *Cfh*$^{-/-}$ *Cfd*$^{-/-}$ mice are high if neither FH nor FD is added. When a single dose of FD is given (1 μg/kg), the minimum concentration of FH required to control complement activity is ~30 μg/mL (arrow). (**F**) Plasma C3 levels vary as a function of the FD/FH ratio. Higher FD/FH ratios are associated with poorer levels of complement control, as reflected by lower levels of C3. (**G**) With increasing levels of FD, higher levels of FH are required to control complement activity. Note that the same amount of FH (plasma concentration of FH for all animals in **G** is ~50 μg/mL) fails to normalize plasma C3 in animals treated with a high dose of FD (100 μg/kg).

## Methods

*Mice*. *Cfh*$^{-/-}$ and *Cfd*$^{-/-}$ mice were generated as previously described (11, 44). After crossing the *Cfd*$^{-/-}$ and *Cfh*$^{-/-}$ mice, *Cfh*$^{+/-}$ *Cfd*$^{+/-}$ progeny were backcrossed to C57BL/6 (stock no. 000664, The Jackson Laboratory) for 10 generations. Littermates of *Cfh*$^{-/-}$, *Cfd*$^{-/-}$, *Cfh*$^{-/-}$ *Cfd*$^{-/-}$, and WT mice were used in all experiments. All study animals had free access to water except during the water-deprivation study (WDS). In the WDS, a mouse in a metabolic cage was deprived of water for 9 hours and then received by intraperitoneally injection a dose (1 μg/kg) of antidiuretic hormone (V0377, Sigma-Aldrich) in 100 μL of saline solution. The injected mouse was then monitored in the metabolic cage for an additional 3 hours. Urine was collected during both periods and osmolarity was measured using a cryo-osmometer.

*Ex vivo studies with patient samples*. Patients enrolled in our C3G biobank from 2010–2019 with biopsy-confirmed C3G were eligible to participate in this study if sufficient sera and plasma were available for the proposed complement assays.

*Western blotting*. Blood from mice was collected from the submandibular vein in the presence of EDTA and immediately separated to collect plasma, which was stored at –80°C. Samples were diluted

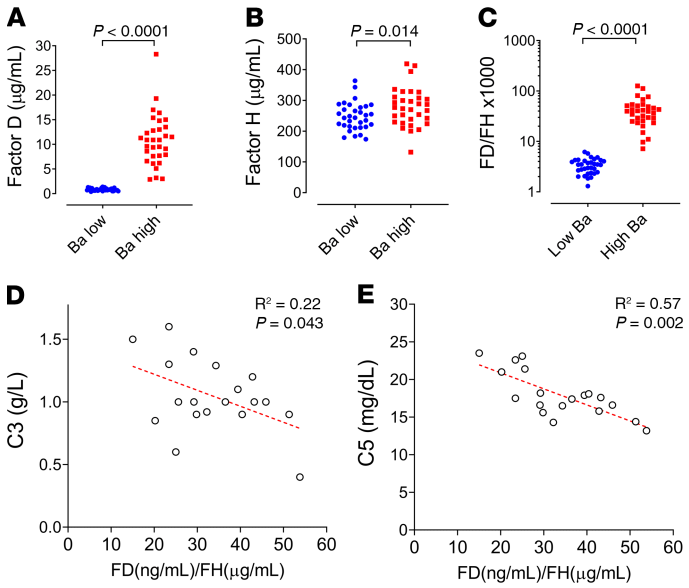


**Figure 8. Plasma FH and FD levels in patients with C3 glomerulopathy.** (**A** and **B**) FD levels are significantly elevated in patients ($n$ = 32) with chronic renal disease as reflected by high Ba compared with patients ($n$ = 33) with normal glomerular filtration rate, as indicated by low Ba (**A**), while FH levels are comparable between groups (**B**). (**C**) FD/FH ratios are significantly increased in patients with chronic renal disease due to the increase of FD. (**D** and **E**) Plasma C3 and C5 in patients with high FD (> 3 μg/mL; normal reference < 2 μg/mL) and without autoantibodies ($n$ = 19). Higher levels of FD are associated with poorer levels of complement control for a given level of FH. The 2-tailed unpaired $t$ test is performed on **A**, **B**, and **C**. Linear regression analysis is performed on **D** and **E**.

1:40 in Laemmli buffer and resolved on an SDS-PAGE gel under reducing conditions for C3 and FB, and under nonreducing condition for C5; gels were transferred to nitrocellulose membranes. Antibody detection was performed as follows: goat anti–mouse C3d (1:2000; AF2655, R&D Systems), goat anti–serum to human FB (1:8000; A311, Quidel), and goat anti–serum to human C5 (1:4000; A306, Quidel), respectively, followed by HRP-conjugated secondary antibodies (Jackson ImmunoResearch). Blots were visualized using Pierce ECL Western Blotting substrate (Thermo Fisher Scientific) and quantified with ImageJ (v1.5 for Windows, NIH).

Tissues (kidney, liver, heart, spleen, lung, brain, and eye) were collected from *Cfh*$^{-/-}$ *Cfd*$^{-/-}$ mouse at various ages and homogenized in liquid nitrogen. Crushed tissues were resuspended in Tissue Extraction Reagent (FNN0071, Thermo Fisher Scientific) and sonicated followed by centrifugation at 10,000 *g* at 4°C for 5 minutes. Proteins were quantified using the BCA Protein Kit (23225, Thermo Fisher Scientific). Twenty-five μg of lysate was loaded on an SDS-PAGE gel; the same Western blot procedure was then followed. Antibody detection was performed using chicken anti–human C3a (1:2000; ab48581, Abcam) and HRP-labeled goat anti–chicken IgG (1:8000; Jackson ImmunoResearch). The same blot was stripped of antibodies and reprobed with rabbit anti–human β-actin (1:10,000; ab16039, Abcam) and HRP-labeled goat anti–rabbit IgG (1:8000; Jackson ImmunoResearch).

*Hemolytic assay*. Rabbit erythrocytes ($1 \times 10^7$) were incubated with 20% mouse serum at 37°C for 45 minutes in EGTA (10 mM)/$Mg^{2+}$(5 mM) buffer or EDTA (10 mM) as a control in a final volume of 100 μL. To stop the reaction, 150 μL of EDTA buffer was added. After centrifugation (1000 *g* for 10 minutes at 25°C), optical density of the supernatant was measured at 415 nm and percent hemolysis was calculated (total lysis by water as 100%). Various SPs or complement regulators were introduced in the assay before adding cells. Tested SPs included PK, FVIIa, FIXa, FXa, FXIa, FXIIa, FXIIIa, thrombin, plasmin and APC (all from Enzyme Research Laboratories). The effect of the PK inhibitor, PKSI-527 (Santa Cruz Biotechnology) was also measured. Tested complement factors and regulators included MASP-3 (R&D Systems), C1s (Abcam), C1-Inh (Complement Technology) and soluble CR1 (Celldex Therapeutics).

*Murine plasma C3, FB, and C5 levels*. Mouse total C3 was assayed using the Mouse Complement C3 Kit (Genway Biotech, San Diego, CA). Plasma concentrations of FB and C5 were estimated from Western

blots using purified human FB and C5 (both from Complement Technology) of known concentration as a reference. All blots were striped and reprobed with anti-G6PD (1:10,000; ab9484, Abcam), which was used as a loading control.

*Human plasma C3, C5, FD, and FH levels*. C3 and FD were measured using human C3 and FD kits, respectively (Hycult). FH was assayed using the MicroVue Factor H kit (Quidel). C5 was quantified by radial immunodiffusion (The Binding Site).

*Survival*. Survival was followed in *Cfh*$^{-/-}$, *Cfd*$^{-/-}$, *Cfh*$^{-/-}$ *Cfd*$^{-/-}$, and WT mice for 10 months and analyzed using the Kaplan-Meier method and Mantel-Cox logrank test.

*Renal immunostaining*. Kidneys were imbedded in OCT freezing medium at the time of sacrifice and sectioned at 10 μM. Sections were fixed in 4% paraformaldehyde for 10 minutes, washed 3 times in PBS, blocked in 10% goat serum (G9023; Sigma-Aldrich) in PBS for 30 minutes and stained using polyclonal C3-FITC–labeled antibody for presence of C3 (1:800; 0855500, MP Biomedicals), rat anti–mouse C3b/C3c/iC3b mAb (1:800; HM1065, Hycult), goat anti–mouse C3d (1:500; AF2655, R&D Systems), C5b-9 (1:800; ab55811, Abcam), and a corresponding FITC-conjugated secondary antibody (Southern Biotech). Images were acquired using a confocal microscope (Zeiss 710). Ten glomeruli were assessed per section.

*Electron microscopy*. Renal cortex (<0.5 $mm^3$) was washed with PBS briefly, fixed with a modified 2.5% Karnovsky's fixative (2.5% glutaraldehyde, 4% paraformaldehyde, and 0.02% picric acid in 0.1M sodium cacodylate buffer at pH 7.2). Samples were postfixed in 1% osmium tetroxide and 1.5% potassium ferricyanide, dehydrated through a graded ethanol series, and embedded in an EPON resin (Electron Microscopy Sciences). Ultrathin sections were cut on a Leica Ultracut S Ultramicrotome (Leica Microsystems), collected on copper grids, post-stained with lead citrate, and viewed on a JEM 1400 electron microscope (JEOL).

*Preparation of C3(MA)*. C3(MA) was prepared by incubating C3 (5 mg/mL, Complement Technology) at 37°C with 1M methylamine ($CH_3NH_2$) at a 1:1 ratio for 2 hours. Following incubation, C3(MA) solution was dialyzed using 10 k dalton dialysis tubes (Thermo Fisher Scientific) with PBS (pH 7.4) overnight.

*Administration of C3, C3(MA), C1-Inh, FH or FD to Cfh*$^{-/-}$ *Cfd*$^{-/-}$ *mice*. To administer C3 or C3(MA), 3-month-old mice received by intraperitoneal injection a single dose of 1.5 mg of C3(MA) or C3 diluted in PBS to a final concentration of 500 μg/mL or an identical volume of PBS. Blood and kidneys were collected 8 hours after injection.

To administer C1-Inh, 2- to 3-month-old animals received by intraperitoneal injection a single dose of Berinert (40 IU /mouse, CSL Behring) or an identical volume of PBS. Blood was collected 20 hours after injection.

To administer FH or FD, 2- to 3-month-old animals received by intraperitoneal injection varying amounts of human FH or FD (both from Complement Technology) or an identical volume of PBS. The dosing ranges were 0.25 to 20 mg/kg for FH and 0.1 to 10 μg/kg for FD. Mice were euthanized at 48 hours following FH injection, or at the indicated time points following FD injection. Blood and renal tissues were collected for analysis.

*Renal function*. Twenty-four–hour urine volumes were collected in metabolic cages. Serum creatinine was analyzed in plasma, and urine albumin was quantified using a mouse albumin ELISA kit according to the manufacturer's instructions (Bethyl Laboratories).

*Renal pathology*. Kidney histology was examined in PAS and trichrome staining, recording glomerular changes as previous reported (45).

*Statistics*. Statistical comparisons were made using GraphPad Prism version 8.2. Specifically, a 2-tailed unpaired or paired Student's *t* test was performed on 2 groups; 1-way ANOVA was performed on > 2 groups. If significant, Tukey post hoc test was followed to determine differences between groups. A *P* value less than 0.05 was considered significant.

*Study approval*. The mouse study was approved by the IACUC of the University of Iowa. For the human study, each patient provided informed consent, which was approved by the IRB of Carver College of Medicine at the University of Iowa. All studies were conducted in accordance with the Declaration of Helsinki.

## Author contributions

YZ and RJHS designed the study and wrote the manuscript. YZ, AK, KSM, EEA, MAL, JBH, and GRP conducted experiments, analyzed data, and interpreted the results. DFD analyzed the pathology. RPT provided reagents, contributed to the experimental design, and revised the manuscript. All authors reviewed and approved the final manuscript.

## Acknowledgments

We would like to thank Matthew Pickering and Yuanyan Xu for the *Cfh*$^{-/-}$ and *Cfd*$^{-/-}$ mice, respectively, and we thank the central microscopy research facility at the University of Iowa for electron microscopic technique assistance. This work was supported by NIH grant R01 DK110023 (RJHS) and K08 HL145138 (DD).

Address correspondence to: Richard J.H. Smith, Molecular Otolaryngology & Renal Research Laboratories, The University of Iowa, 285 Newton Road, 5270 CBRB, Iowa City, Iowa 52242-1078, USA. Phone: 319.335.6623; Email: richard-smith@uiowa.edu.

1. Hillmen P, et al. Effect of eculizumab on hemolysis and transfusion requirements in patients with paroxysmal nocturnal hemoglobinuria. *N Engl J Med*. 2004;350(6):552–559.
2. Rother RP, Rollins SA, Mojcik CF, Brodsky RA, Bell L. Discovery and development of the complement inhibitor eculizumab for the treatment of paroxysmal nocturnal hemoglobinuria. *Nat Biotechnol*. 2007;25(11):1256–1264.
3. Dmytrijuk A, Robie-Suh K, Cohen MH, Rieves D, Weiss K, Pazdur R. FDA report: eculizumab (Soliris) for the treatment of patients with paroxysmal nocturnal hemoglobinuria. *Oncologist*. 2008;13(9):993–1000.
4. Loirat C, Frémeaux-Bacchi V. Atypical hemolytic uremic syndrome. *Orphanet J Rare Dis*. 2011;6:60.
5. Smith RJH, et al. C3 glomerulopathy - understanding a rare complement-driven renal disease. *Nat Rev Nephrol*. 2019;15(3):129–143.
6. Bomback AS, et al. Eculizumab for dense deposit disease and C3 glomerulonephritis. *Clin J Am Soc Nephrol*. 2012;7(5):748–756.
7. Le Quintrec M, et al. Patterns of Clinical Response to Eculizumab in Patients With C3 Glomerulopathy. *Am J Kidney Dis*. 2018;72(1):84–92.
8. Götze O, Müller-Eberhard HJ. The c3-activator system: an alternate pathway of complement activation. *J Exp Med*. 1971;134(3):90–108.
9. Lesavre PH, Müller-Eberhard HJ. Mechanism of action of factor D of the alternative complement pathway. *J Exp Med*. 1978;148(6):1498–1509.
10. Volanakis JE, Barnum SR, Giddens M, Galla JH. Renal filtration and catabolism of complement protein D. *N Engl J Med*. 1985;312(7):395–399.
11. Pickering MC, et al. Uncontrolled C3 activation causes membranoproliferative glomerulonephritis in mice deficient in complement factor H. *Nat Genet*. 2002;31(4):424–428.
12. Pangburn MK, Schreiber RD, Müller-Eberhard HJ. Formation of the initial C3 convertase of the alternative complement pathway. Acquisition of C3b-like activities by spontaneous hydrolysis of the putative thioester in native C3. *J Exp Med*. 1981;154(3):856–867.
13. Pangburn MK. The Alternative Pathway. In: Ross GD, ed. *Immunobiology of the Complement System*. Orlando, FL: Academic Press; 1986:21–44.
14. Abrera-Abeleda MA, Xu Y, Pickering MC, Smith RJ, Sethi S. Mesangial immune complex glomerulonephritis due to complement factor D deficiency. *Kidney Int*. 2007;71(11):1142–1147.
15. DiLillo DJ, et al. Selective and efficient inhibition of the alternative pathway of complement by a mAb that recognizes C3b/iC3b. *Mol Immunol*. 2006;43(7):1010–1019.
16. Frei Y, Lambris JD, Stockinger B. Generation of a monoclonal antibody to mouse C5 application in an ELISA assay for detection of anti-C5 antibodies. *Mol Cell Probes*. 1987;1(2):141–149.
17. Björkqvist J, Jämsä A, Renné T. Plasma kallikrein: the bradykinin-producing enzyme. *Thromb Haemost*. 2013;110(3):399–407.
18. DiScipio RG. The activation of the alternative pathway C3 convertase by human plasma kallikrein. *Immunology*. 1982;45(3):587–595.
19. Irmscher S, et al. Kallikrein Cleaves C3 and Activates Complement. *J Innate Immun*. 2018;10(2):94–105.
20. Jiang H, Wagner E, Zhang H, Frank MM. Complement 1 inhibitor is a regulator of the alternative complement pathway. *J Exp Med*. 2001;194(11):1609–1616.
21. Hack CE, Paardekooper J, Van Milligen F. Demonstration in human plasma of a form of C3 that has the conformation of "C3b-like C3". *J Immunol*. 1990;144(11):4249–4255.
22. Oppermann M, Kurts C, Zierz R, Quentin E, Weber MH, Götze O. Elevated plasma levels of the immunosuppressive complement fragment Ba in renal failure. *Kidney Int*. 1991;40(5):939–947.
23. Vernon KA, Ruseva MM, Cook HT, Botto M, Malik TH, Pickering MC. Partial Complement Factor H Deficiency Associates with C3 Glomerulopathy and Thrombotic Microangiopathy. *J Am Soc Nephrol*. 2016;27(5):1334–1342.
24. Alexander JJ, et al. Mouse podocyte complement factor H: the functional analog to human complement receptor 1. *J Am Soc Nephrol*. 2007;18(4):1157–1166.
25. Law SKA, Levine RP. The covalent binding story of the complement proteins C3 and C4 (I) 1972-1981. *Immunobiology*. 2019;224(6):827–833.
26. Ekdahl KN, et al. Is generation of C3($H_2O$) necessary for activation of the alternative pathway in real life? *Mol Immunol*. 2019;114:353–361.
27. Sohn JH, Bora PS, Suk HJ, Molina H, Kaplan HJ, Bora NS. Tolerance is dependent on complement C3 fragment iC3b binding to antigen-presenting cells. *Nat Med*. 2003;9(2):206–212.
28. Torreira E, Tortajada A, Montes T, Rodríguez de Córdoba S, Llorca O. Coexistence of closed and open conformations of complement factor B in the alternative pathway C3bB(Mg2+) proconvertase. *J Immunol*. 2009;183(11):7347–7351.
29. Hiemstra PS, et al. Complete and partial deficiencies of complement factor D in a Dutch family. *J Clin Invest*. 1989;84(6):1957–1961.
30. Biesma DH, et al. A family with complement factor D deficiency. *J Clin Invest*. 2001;108(2):233–240.
31. Sprong T, et al. Deficient alternative complement pathway activation due to factor D deficiency by 2 novel mutations in the

complement factor D gene in a family with meningococcal infections. *Blood*. 2006;107(12):4865–4870.
32. Sng CCT, et al. A type III complement factor D deficiency: Structural insights for inhibition of the alternative pathway. *J Allergy Clin Immunol*. 2018;142(1):311–314.e6.
33. Rusai K, et al. A rare case: childhood-onset C3 glomerulonephritis due to homozygous factor H deficiency. *CEN Case Rep*. 2013;2(2):234–238.
34. Servais A, et al. Heterogeneous pattern of renal disease associated with homozygous factor H deficiency. *Hum Pathol*. 2011;42(9):1305–1311.
35. Cho HY, Lee BS, Moon KC, Ha IS, Cheong HI, Choi Y. Complete factor H deficiency-associated atypical hemolytic uremic syndrome in a neonate. *Pediatr Nephrol*. 2007;22(6):874–880.
36. Vaziri-Sani F, et al. Phenotypic expression of factor H mutations in patients with atypical hemolytic uremic syndrome. *Kidney Int*. 2006;69(6):981–988.
37. Licht C, et al. Successful plasma therapy for atypical hemolytic uremic syndrome caused by factor H deficiency owing to a novel mutation in the complement cofactor protein domain 15. *Am J Kidney Dis*. 2005;45(2):415–421.
38. Dragon-Durey MA, et al. Heterozygous and homozygous factor h deficiencies associated with hemolytic uremic syndrome or membranoproliferative glomerulonephritis: report and genetic analysis of 16 cases. *J Am Soc Nephrol*. 2004;15(3): 787–795.
39. Lopez Larrea C, et al. A familial deficiency of complement factor H. *Biochem Soc Trans*. 1987;15(4):648–649.
40. Barbour TD, Pickering MC, Terence Cook H. Dense deposit disease and C3 glomerulopathy. *Semin Nephrol*. 2013;33(6):493–507.
41. Pascual M, Paccaud JP, Macon K, Volanakis JE, Schifferli JA. Complement activation by the alternative pathway is modified in renal failure: the role of factor D. *Clin Nephrol*. 1989;32(4):185–193.
42. Carpenter CB, Ruddy S, Shehadeh IH, Müller-Eberhard HJ, Merrill JP, Austen KF. Complement metabolism in man: hyper-catabolism of the fourth (C4) and third (C3) components in patients with renal allograft rejection and hereditary, angioedema (HAE). *J Clin Invest*. 1969;48(8):1495–1505.
43. Hugo F, Berstecher C, Krämer S, Fassbender W, Bhakdi S. In vivo clearance studies of the terminal fluid-phase complement complex in rabbits. *Clin Exp Immunol*. 1989;77(1):112–116.
44. Xu Y, Ma M, Ippolito GC, Schroeder HW, Carroll MC, Volanakis JE. Complement activation in factor D-deficient mice. *Proc Natl Acad Sci USA*. 2001;98(25):14577–14582.
45. Lesher AM, et al. Combination of factor H mutation and properdin deficiency causes severe C3 glomerulonephritis. *J Am Soc Nephrol*. 2013;24(1):53–65.